Supplementary information

Decadal-scale decay of landslide-derived fluvial suspended sediment after Typhoon Morakot

Gregory Ruetenik[1], Ken L. Ferrier[2], and Odin Marc[3]

[1] Institute of Geophysics, Czech Academy of Sciences, Prague, Czech Republic
[2] Department of Geoscience, University of Wisconsin-Madison, Madison, WI, USA
[3] Geosciences Environnement Toulouse, France

Overview

The supplementary tables contain information about the suspended sediment monitoring data at the fluvial gauging stations and the landslide characteristics inside the drainage basins above them. These are contained as spreadsheets in a separate supplementary data file.

Table S1: Gauging station locations, IDs, drainage basin areas, duration of monitoring, and nested gauging stations
Table S2: Pre-Morakot values of rating curve parameters $\tilde{a}_{pre}$ and b_{pre}, basin-averaged landslide intensity, characteristic decay times of $\tilde{a}$
Table S3: Annual values of the rating curve parameter $\tilde{a}$
Table S4: Annual values of the rating curve parameter b
Table S5: Annual values of the suspended sediment discharge Q_s

Figure S1 shows the probability distributions of mean daily discharge for the North and South focus stations based on all historical data, while Figure S2 shows the maximum discharge in each year since 1990. Figure S3 shows a figure analogous to Figure 8 in the main text, plotting ΔQ_s against Morakot-induced precipitation, while Figure S4 shows an analagous figure to Figure 10 of the main text, plotting regression slopes and τ_a against Morakot-induced precipitation. Figures S5 and S6 contain the changes in the rating curve parameters relative to their pre-Morakot values for each year after Morakot. Regression slopes through these annual datasets are summarized in Figure 11 in the main text.

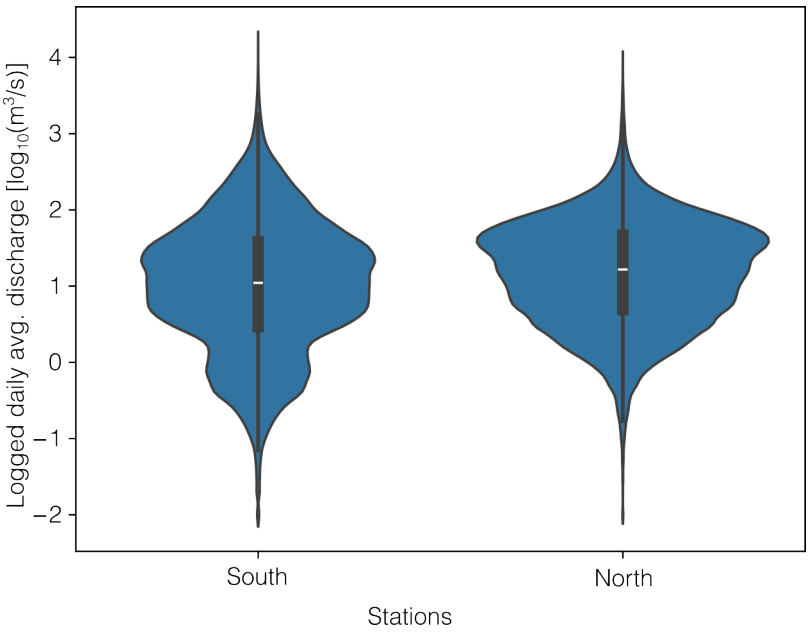

Figure S1. Comparison of daily average discharge for the northern and southern focus stations over the entire historical record. The violin plots (a symmetric probability distribution) show that the frequency distributions of discharge are similar at the northern and southern focus stations.

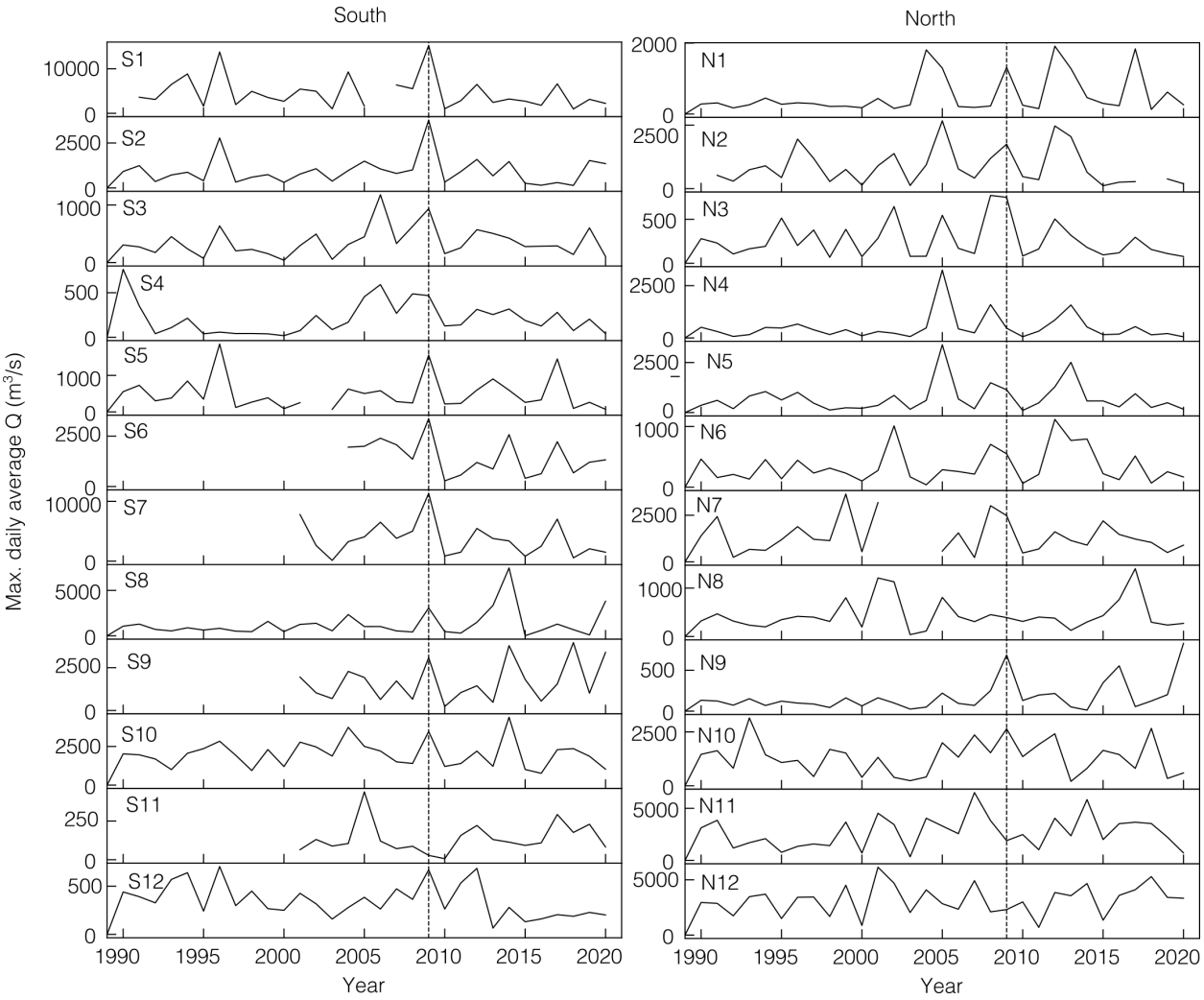

Figure S2: Maximum daily average discharge each year from 1990 to 2020 for the northern and southern focus stations. The discharge corresponding to Morakot (vertical dashed line) is one of the larger events on record for many of the southern stations. At the northern stations, by contrast, many stations show a peak corresponding to Morakot, but it is less pronounced.

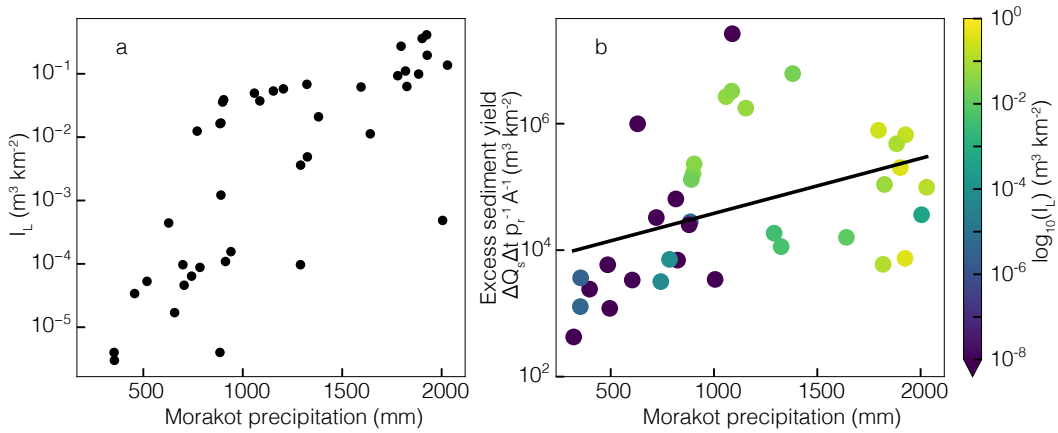

Figure S3: a) Morakot precipitation plotted against landslide intensity, showing a positive correlation. b) Excess sediment yield, as in Figure 8, plotted against Morakot basin-averaged precipitation. This demonstrates a modest correlation between excess sediment yield and Morakot precipitation.

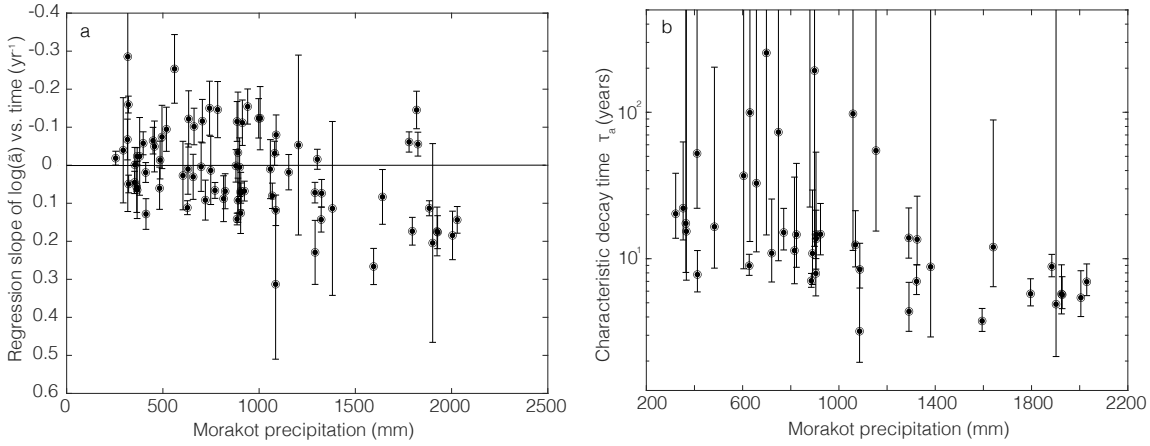

Figure S4a: Regression slope of ln(ã) vs. time (as in Figure 10) against Morakot basin-averaged precipitation. **b**. Characteristic decay time τ_a against Morakot basin-averaged precipitation.

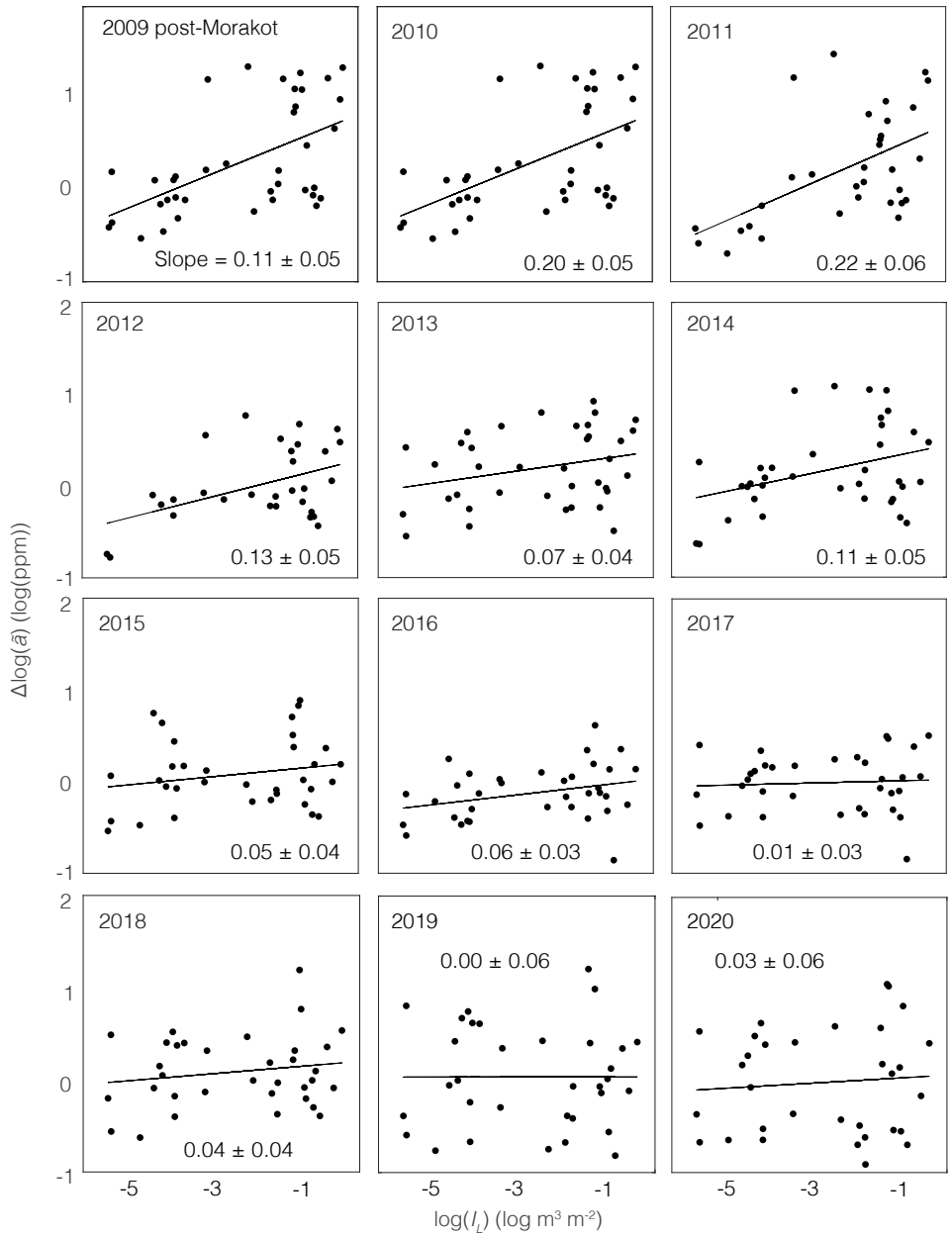

Figure S5. Sensitivity of changes in $\tilde{a}$ to the intensity of Morakot-induced landslides I_L. $\Delta\log(\tilde{a})$ is the difference between $\log(\tilde{a})$ at a given time after Morakot relative to its value before Morakot. E.g., in the upper left panel, $\Delta\log(\tilde{a})$ is $\log(\tilde{a})$ in the post-Morakot portion of 2009 minus $\log(a_{pre})$. Values in each panel are mean ± standard error of the slope of the regression. These are the same values summarized in Figure 11b in the main text.

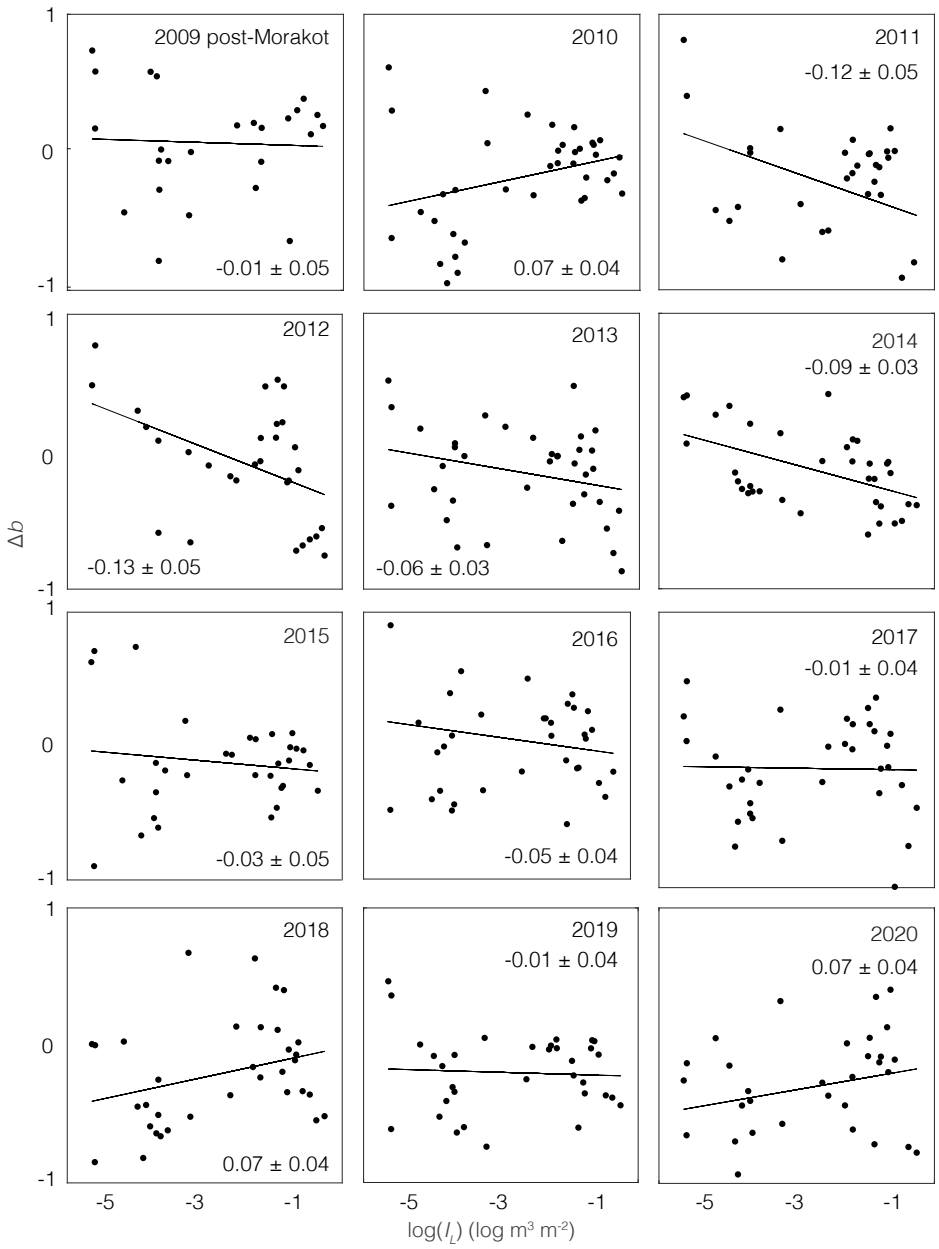

Figure S6. Sensitivity of changes in b to the intensity of Morakot-induced landslides I_L. Δb is the difference between b at a given time after Morakot relative to its value before Morakot. E.g., in the upper left panel, Δb is b in the post-Morakot portion of 2009 minus b_{pre}. Values in each panel are mean ± standard error of the slope of the regression. These are the same values summarized in Figure 11d in the main text.